ACS Macro Letters

Letter

pubs.acs.org/macroletters

Evidence of Cybotactic Order in the Nematic Phase of a Main-Chain Liquid Crystal Polymer with Bent-Core Repeat Unit

Francesco Vita,[†] Katia Sparnacci,[‡] Guido Panzarasa,[‡] Immacolata F. Placentino,[†] Salvatore Marino,[§] Nicola Scaramuzza,[§] Giuseppe Portale,[$] Emanuela Di Cola,[∥] Claudio Ferrero,[∥] Sofia I. Torgova,[⊥] Giancarlo Galli,[#] Michele Laus,[‡] and Oriano Francescangeli*[,†]

[†]Dipartimento SIMAU and CNISM, Università Politecnica delle Marche, via Brecce Bianche, 60131 Ancona, Italy

[‡]Dipartimento DISIT, Università del Piemonte Orientale "A. Avogadro", INSTM, UdR Alessandria, Via T. Michel 11, 15121 Alessandria, Italy

[§]Dipartimento di Fisica, Università della Calabria, CNR-IPCF UoS Cosenza, Licryl Laboratory, and Centro di Eccellenza CEMIF.CAL, Via Pietro Bucci, Cubo 31C, 87036 Rende, Cosenza, Italy

[∥]European Synchrotron Radiation Facility, Boîte Postale 220, 38043 Grenoble Cedex, France

[⊥]P.N. Lebedev Physical Institute of the Russian Academy of Sciences, Leninsky Pr. 53, Moscow, 119991 Russia

[#]Dipartimento di Chimica e Chimica Industriale, Università di Pisa, INSTM, UdR Pisa, Via Risorgimento 35, I-56126 Pisa, Italy

[$]Netherlands Organization for Scientific Research (NWO), DUBBLE CRG at the ESRF, 6 rue Jules Horowitz, 38043 Grenoble Cedex, France

Supporting Information

ABSTRACT: We report the synthesis and structural characterization of a main-chain liquid crystal polymer constituted by a 1,2,4-oxadiazole-based bent-core repeat unit. For the first time, a liquid crystal polymer made of bent mesogenic units is demonstrated to exhibit cybotactic order in the nematic phase. Coupled with the chain-bond constraints, cybotaxis results in maximized molecular correlations that make this material of great potential in the search for the elusive biaxial and ferroelectric nematic phases. Indeed, repolarization current measurements in the nematic phase hint at a ferroelectric-like switching response (upon application of an electric field of only 1.0 V μm^{-1}) that, albeit to be definitely confirmed by complementary techniques, is strongly supported by the comparative repolarization current measurements in the nematic and isotropic phases. Finally, the weak tendency of this polymer to crystallize makes it possible to supercool the cybotactic nematic phase down to room temperature, thus, paving the way for a glassy phase in which the biaxial (and possibly polar) order is frozen at room temperature.

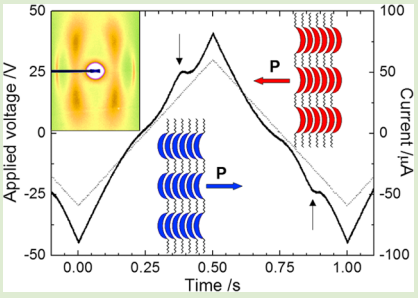

The introduction of mesogenic groups into macromolecular architectures is well-known to lead to special materials in which typical properties of polymers, such as elasticity, mechanical stability, and easy processability, are coupled with liquid crystal (LC) features, such as long-range cooperative effects. Notwithstanding this, research on polymers containing bent mesogenic groups is still limited and mainly focused on side-chain systems,[1] with a few main-chain polymers being also studied.[2] Polar smectic (Sm) phases (*banana phases*)[3] analogous to those encountered in low molecular weight bent-core mesogens (BCMs) were described, although high viscosity and high phase transition temperatures, observed especially for main chain polymers, often hindered ferroelectric switching and restricted detailed investigations. By contrast, there are no reports on the nematic (N) phase of this class of macromolecules.

In recent years the N phase of low molecular weight BCMs has attracted growing interest because of its unconventional properties[4] and the evidence of extraordinary effects.[5] In particular, BCMs have gained the role of leading candidates in the long-lasting search for the elusive biaxial and ferroelectric thermotropic N phases. Biaxiality was first reported in a 1,3,4-oxadiazole-based BCM in 2004,[6] although its very nature (spontaneous vs induced; local vs macroscopic) is still controversial.[7] On the other hand, the first observation of ferroelectric switching in thermotropic nematics was reported in 2009 by Francescangeli et al.[8a] for the BCM 3,5-bis-{4-[4-(*n*-nonyloxy)benzoyloxy]phenyl}-1,2,4-oxadiazole (**I**), whose structure is shown in Scheme 1A and lately confirmed by Shanker et al.[8b] for other 1,2,4-oxadiazole-based BCMs and very recently by Ghosh et al. for asymmetric four-ring BCMs.[8c]

Although the scientific debate on these topics is ongoing, there is now a general consensus that the unconventional behavior of bent-core nematics is due to the cybotactic nature

Received: October 8, 2013
Accepted: December 26, 2013
Published: December 31, 2013

Scheme 1. Chemical Structures of Compounds (A) I and (B) II; (C) Synthetic Route to Polymer II

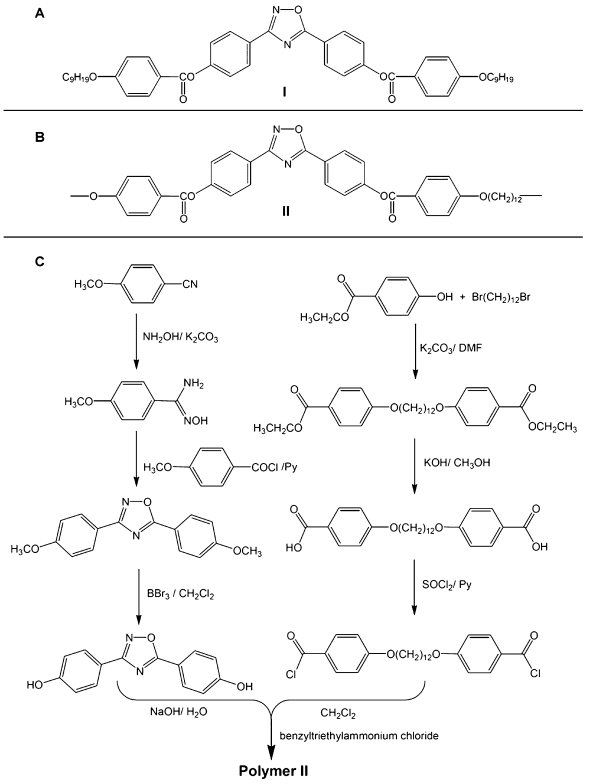

of the N phase, that is, the existence of nanometer-sized biaxial, and possibly polar, clusters (cybotactic groups) characterized by a short-range (generally skewed) Sm-like order.[4,5,7−10] These clusters, which persist all over the N temperature range, are now widely recognized as an inherent feature of the N phase of BCMs, and accordingly, the phase is generally referred to as the cybotactic N (N_{cyb}) phase. In the case of **I**, X-ray diffraction (XRD) studies, repolarization current measurements, and electro-optical characterization combined with molecular dynamics simulations, have shown that the clusters' polar axes, transversal to the long axis molecular director **n**, are randomly oriented in the absence of an electric field **E**, so that the material is macroscopically uniaxial and the macroscopic polarization averages to zero. However, an external **E** field above a certain threshold is able to align the clusters' polar axes over macroscopic volumes, causing a transition to a biaxial ferroelectric state characterized by a macroscopic polarization of 10−100 nC cm^{-2} (depending on the temperature) that can be reversed by changing the sign of **E**. Once this polar state has settled, the switching takes place through the cooperative rotation of the BCMs of each group about their long molecular axis.[8a]

Inspired by these results, we have recently undertaken the study of thermotropic main chain LC polymers made of bent-core monomeric units, with the aim of exploring the extent to which the cybotactic order (and resulting properties) can be translated to the N phase of these materials. Here we report the synthesis and structural characterization of a polymeric counterpart of BCM **I**, that is, a LC polymer (**II**) featuring a regular alternation of 1,2,4-oxadiazole-based bent mesogenic cores and dodecamethylene spacers (Scheme 1B). We show for the first time how cybotactic order dominates the N phase of a polymeric BCM and demonstrate the possibility of supercooling the cybotactic nematic down to room temperature (RT) in the glassy phase. Compared to low molecular weight BCMs, chain-bond constraints can enhance cluster orientational correlations, making polymeric BCMs very promising materials in the search for biaxiality and ferroelectricity in the N phase.

The reaction pathway leading to **II** is outlined in Scheme 1C (see Supporting Information for further details). Polymer **II** shows a multiple melting transition on heating, with a final melting temperature of 177 °C, and a supercooling of recrystallization on cooling (Supporting Information, Figure S1). The isotropization appears as a wide peak with maximum at 278 °C (enthalpy change ΔH = 4.2 J g^{-1}), although at high temperature some degradation occurs; a glass transition is observed at T_g = 44 °C. In the temperature region comprised between melting and isotropization, typical N schlieren textures (with 2- and 4-brush disclinations) are observed (inset of Figure S1).

An extensive XRD study was performed on the ID02 (low-angle XRD) and BM26B (wide-angle XRD) beamlines at the European Synchrotron Radiation Facility (ESRF) to investigate the structure of the N phase of **II** (see Supporting Information). Figure 1A−K shows a representative selection of low-angle (LA) XRD patterns collected over a full thermal cycle with the sample subjected to a horizontal aligning magnetic field B = 1 T. The LA-XRD study was complemented by wide-angle (WA) XRD measurements in order to explore the mesophase structure up to the scale of tenths of a nanometer. A representative selection of the WA-XRD patterns collected on cooling the magnetically aligned sample down from T = 230 °C is shown in Figure 2A−F, together with the corresponding azimuthally integrated intensities (Figure 2G).

On heating (Figure 1A−F), the transition from the low temperature crystal phase becomes apparent above 200 °C; at T = 205 °C a clear diffuse four-spot pattern is observed, associated with the onset of the N phase, together with a couple of weaker sharp meridional peaks (Figure 1A) whose origin will be considered below. As discussed in previous papers,[8a,10] four-spot patterns like those observed in Figures 1 and 2 are the signature of the skewed, SmC-like, N_{cyb} phase of BCMs. The WA diffuse crescents (Figure 2A) centered on the equatorial axis (i.e., perpendicular to the meridional **B** field) indicate that the BCMs align, on average, with their long axes (hence, the molecular director **n**) parallel to **B**, in agreement with the positive diamagnetic anisotropy of the mesogen.

Quantitative analysis of the four-spot pattern provides the structural features relevant to the cybotactic order:[10b] the scattering vector $\mathbf{q_0}$ of the four-spot maxima gives the spacing $d = 2\pi/q_0$ of the Sm layers in the cybotactic clusters, whereas the angle β between $\mathbf{q_0}$ and **B** gives the average tilt angle of the BCM long molecular axes with respect to the Sm layer normal. Figure 1L shows the temperature behavior of d, β, and the calculated length L of the BCM repeat unit, $L = d/\cos\beta$, over a full heating−cooling thermal cycle. As previously observed in other BCMs,[8a,10b,c,f] d and β exhibit a pronounced temperature dependence (with opposite sign), whereas L remains essentially constant over the entire N range. This has been recognized as an indisputable proof of the skewed cybotactic nature of the N phase.[10b,c] The value $L \approx 39$ Å calculated from XRD data (Figure 1L) fits well the length of the repeat unit deduced from molecular dynamics simulations,[8a,10b] $L_{MD} \approx 40$ Å. The center of the WA diffuse crescents corresponds to a spacing $D \approx 4.5$ Å,

dx.doi.org/10.1021/mz400518x | ACS Macro Lett. 2014, 3, 91−95

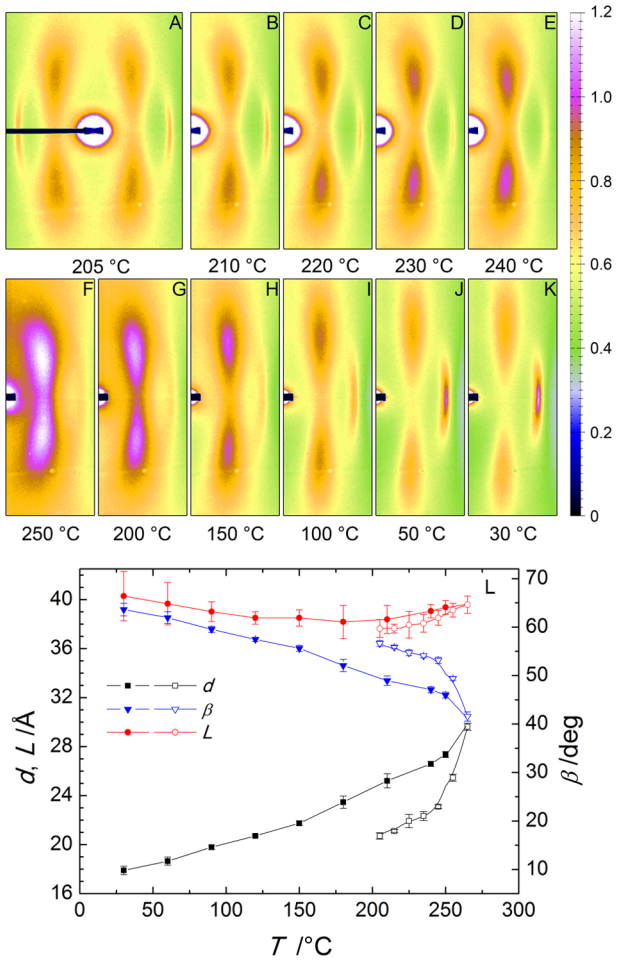

Figure 1. LA-XRD patterns of **II** collected on (A–F) heating and (G–K) cooling the sample under a horizontal aligning **B** field. (L) Temperature dependence of the XRD structural parameters on heating (empty symbols) and cooling (full symbols): d is the layer spacing (black squares), β the tilt angle (blue triangles), and $L = d/\cos\beta$ the calculated molecular length (red circles).

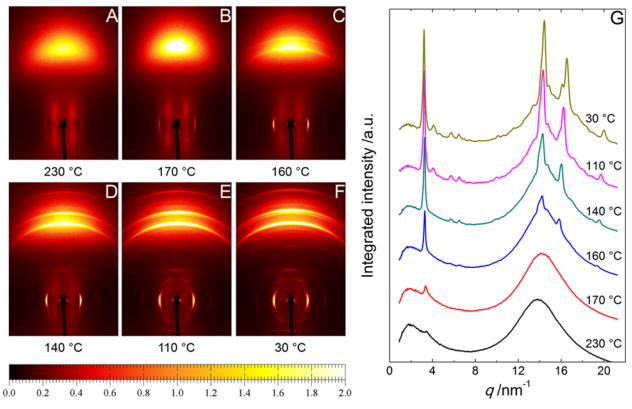

Figure 2. (A–F) WA-XRD diffraction patterns of **II** collected on cooling from the N_{cyb} phase (T = 230 °C) under a horizontal aligning **B** field; because of the symmetry of the pattern, only the upper half is entirely shown. (G) Corresponding q-scans obtained by azimuthal integration.

which represents the average interchain distance in the transversal (⊥ **n**) plane.

The size of the cybotactic clusters was estimated via the longitudinal (∥ **B**) and transversal (⊥ **B**) positional correlations lengths, $\xi_{\parallel}$ and $\xi_{\perp}$, featuring the short-range SmC-like ordering within the clusters. The correlation lengths were calculated as $\xi_{\parallel} = 2/\Delta q_{\parallel}$ and $\xi_{\perp} = 2/\Delta q_{\perp}$, where $\Delta q_{\parallel}$ and $\Delta q_{\perp}$ are the full widths at half-maximum of the lineshapes fitting the intensity profiles of the LA peaks, parallel and orthogonal to **B** respectively.[8a,10b] This procedure gave values of $\xi_{\parallel} \approx L$, that is, of the order of the repeat unit length, and $\xi_{\perp} \approx \xi_{\parallel}/2$, of the order of a few transversal interchain distances (D), very similar to those found in the low molar mass BCM **I**.[8a] Accordingly, the cybotactic clusters consist of nanometer sized domains, including a number of BCM units of the order of a hundred.

Concerning the LA sharp meridional features accompanying the four-spot pattern, a close inspection of Figures 1 and 2 reveals that their origin is unrelated to the N_{cyb} ordering. In fact, on increasing temperature (Figure 1A–F), the four-spot pattern strengthens, whereas the meridional peaks gradually fade until virtually disappearing at temperatures above 250 °C. A similar behavior is reversibly observed on cooling (Figures 1G–K and 2), with the major recovery of these peaks occurring at temperatures below 160 °C, corresponding to the onset of recrystallization. Their maxima in the q-space are essentially constant with temperature (Figure 2G) and correspond to a d-spacing of ∼19.5 Å, that is, half the monomer length L. Accordingly, these weak LA features appear to originate from a residual tendency of the polymeric chains to align parallel to form an intercalated structure in which they are statistically shifted to each other by $L/2$. This tendency is inherently stronger at low temperatures, consistent with the marked intercalated layered structure of the crystal phase (Figure 2G), and is gradually lost as the temperature increases. We attribute the coexistence, within the N phase, of the dominant skewed cybotactic ordering with the residual intercalated layering of the chains to an effect of the molar mass dispersity of the sample, typical of a step-growth polymer.[11]

Finally, the XRD data (Figures 1K and 2F,G) show that the four-spot pattern persists down to 30 °C, which is a clear indication that the N_{cyb} phase of **II** can be supercooled to RT below T_g. Figure 2G (T = 30 °C) shows that the volume fraction of the supercooled N_{cyb} phase (estimated from the ratio of the integrated intensity of the background diffuse scattering to the total integrated diffracted/scattered intensity) is quite comparable to that of the crystal phase. To the best of our knowledge, this represents the first example of N_{cyb} phase of a bent-core LC polymer, frozen at RT below T_g.

Once the cybotactic nature of the N phase of **II** was established, we performed repolarization current measurements[12] to check for the presence of a ferroelectric-like response similar to that observed in BCM **I**. Measurements were performed on a 30 μm thick cell with a 0.35 cm^2 indium–tin oxide electrode area. Planar alignment was assured by a thin (150 Å) SiO_x film, obliquely evaporated (60°) on the inner cell surfaces.[13] In contrast to aligning polymer coatings, SiO_x deposition was found to prevent parasitic current responses to applied electric fields (see Supporting Information), for example, those due to free charge adsorption/desorption processes. A low-frequency (f = 1 Hz) triangular voltage waveform was applied across the cell, and the generated current was measured on a high precision resistor connected in series with the sample and the voltage generator. Figure 3 shows representative examples of the response curve, measured at T = 248 °C and T = 216 °C with a peak-to-peak driving voltage V_{pp}

dx.doi.org/10.1021/mz400518x | ACS Macro Lett. 2014, 3, 91–95

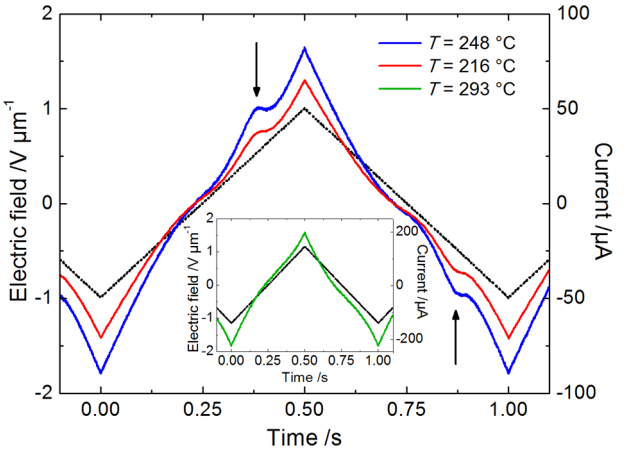

Figure 3. Repolarization current response in the N_{cyb} phase of **II** measured on a 30 μm thick cell at 248 °C (blue solid line) and 216 °C (red solid line) upon application of a triangular wave voltage (f = 1 Hz, V_{pp} = 60 V, black dotted line). The two arrows indicate the current peaks associated with the polarization switching. In the inset, the same measurement performed in the isotropic phase (293 °C, green solid line) with V_{pp} = 70 V.

= 60 V, corresponding to an electric field amplitude E of 1 V μm^{-1}. Two peaks, one per half cycle of the input wave voltage, clearly emerge (with opposite sign) from the linear ohmic background generated by the ionic flow, delayed with respect to the zero-crossing point of the voltage waveform. Similar to what was found in low molar mass LCs,[8] these peaks are consistent with a ferroelectric-like switching, generated by the reversal of a macroscopic electric polarization **P** having a lifetime longer than the half-period of the voltage waveform.[12] A similar behavior was observed with V_{pp} voltages as low as 30 V, that is, with E = 0.5 V μm^{-1}. Although in principle the observed peaks could originate from undesired effects such as sample impurities or surface effects, the observation that the peaks disappear in the isotropic phase (see inset of Figure 3) provides strong evidence against such spurious contributions. Accordingly, by integrating the current peak and dividing by twice the electrode area we estimated the intensity of the polarization to be P = 0.49 ± 0.04 $\mu C\ cm^{-2}$ at T = 216 °C and P = 0.85 ± 0.07 $\mu C\ cm^{-2}$ at T = 248 °C. These values are about 1 order of magnitude larger than those measured in the N_{cyb} phase of **I** and other oxadiazole-based low molecular weight BCMs ($P \leq$ 0.10 $\mu C\ cm^{-2}$ upon application of an electric field of a few V μm^{-1}),[8a,b] as well as in the polar Sm phases of different bent-core LC polymers (0.10−0.50 $\mu C\ cm^{-2}$).[1,2] However, these latter compounds either did not exhibit any switching response[1b,2a] or instead required a significantly larger field ($\geq$10 V μm^{-1}) to reverse the polarization direction.[1a,2b]

In conclusion, this paper provides the first experimental evidence of cybotactic order in the N phase of a LC polymer based on a bent-core monomer. Similarly to the low molar mass BCMs, the cybotactic groups are nanometer-sized and contain a number of monomer units of the order of few hundreds. We have found that the low tendency of this polymeric material to crystallize makes it possible to supercool the N_{cyb} phase down to RT, paving the way for a glassy phase in which the polar order is frozen at RT. The experimental evidence hints at a ferroelectric-like switching response in the N_{cyb} phase that, while to be definitely confirmed by complementary techniques (in particular, second harmonic generation measurements), is strongly supported by the comparative repolarization current measurements in the nematic and isotropic phases. The corresponding macroscopic polarization of **II** is 1 order of magnitude larger than that of BCM **I**. As the average size of the cybotactic groups is the same in **II** and **I**, the enhanced polarization of **II** is to be attributed to the polymeric nature of the material, that is, to the effects of intrachain bonds that strengthen the dipolar orientational correlation among the cybotactic clusters. Once definitely confirmed, the large polarization value and the relatively low switching field of this material (due to the rather fluid nature of the N phase compared to the more solid-like Sm phases) would open new perspectives for innovative applications in the fields of polymeric ferroelectric devices.[14]

■ ASSOCIATED CONTENT

Supporting Information

Synthesis of **II**, its characterization by differential scanning calorimetry and polarization optical microscopy, XRD experimental details, and effect of aligning layers on repolarization current measurements. This material is available free of charge via the Internet at http://pubs.acs.org.

■ AUTHOR INFORMATION

Corresponding Author

*E-mail: o.francescangeli@univpm.it.

Notes

The authors declare no competing financial interest.

■ ACKNOWLEDGMENTS

We acknowledge J. Gorini, M. Fernandez Martinez, and T. Narayanan, ESRF, D. Hermida Merino and W. Bras, Dubble CRG/ESRF, NWO, and F. Vaccaro, Università Politecnica delle Marche, for their support.

■ REFERENCES

(1) (a) Keith, C.; Reddy, R. A.; Tschierske, C. *Chem. Commun.* **2005**, 871. (b) Chen, X.; Tenneti, K. K.; Li, C. Y.; Bai, Y.; Wan, X.; Fan, X.; Zhou, Q.-F.; Rong, L.; Hsiao, B. S. *Macromolecules* **2007**, *40*, 840.

(2) (a) Choi, E.-J.; Ahn, J.-C.; Chien, L.-C.; Lee, C.-K.; Zin, W.-C.; Kim, D.-C.; Shin, S.-T. *Macromolecules* **2004**, *37*, 71. (b) Choi, E.-J.; Kim, E.-C.; Ohk, C.-W.; Zin, W.-C.; Lee, J.-H.; Lim, T.-K. *Macromolecules* **2010**, *43*, 2865.

(3) (a) Niori, T.; Sekine, T.; Watanabe, J.; Furukawa, T.; Takezoe, H. *J. Mater. Chem.* **1996**, *6*, 1231. (b) Takezoe, H.; Takanishi, Y. *Jpn. J. Appl. Phys.* **2006**, *45*, 597. (c) Eremin, A.; Jákli, A. *Soft Matter* **2013**, *9*, 615.

(4) Jákli, A. *Liq. Cryst. Rev.* **2013**, *1*, 65.

(5) (a) Harden, J.; Mbanga, B.; Éber, N.; Fodor-Csorba, K.; Sprunt, S.; Gleeson, J. T.; Jákli, A. *Phys. Rev. Lett.* **2006**, *97*, 157802. (b) Bailey, C.; Fodor-Csorba, K.; Verduzco, R.; Gleeson, J. T.; Sprunt, S.; Jákli, A. *Phys. Rev. Lett.* **2009**, *103*, 237803. (c) Francescangeli, O.; Vita, F.; Fauth, F.; Samulski, E. T. *Phys. Rev. Lett.* **2011**, *107*, 207801. (d) Vita, F.; Placentino, I. F.; Ferrero, C.; Singh, G.; Samulski, E. T.; Francescangeli, O. *Soft Matter* **2013**, *9*, 6475.

(6) (a) Madsen, L. A.; Dingemans, T. J.; Nakata, M.; Samulski, E. T. *Phys. Rev. Lett.* **2004**, *92*, 145505. (b) Acharya, B. R.; Primak, A.; Kumar, S. *Phys. Rev. Lett.* **2004**, *92*, 145506.

(7) Tschierske, C.; Photinos, D. J. *J. Mater. Chem.* **2010**, *20*, 4263.

(8) (a) Francescangeli, O.; Stanic, V.; Torgova, S. I.; Strigazzi, A.; Scaramuzza, N.; Ferrero, C.; Dolbnya, I. P.; Weiss, T. M.; Berardi, R.; Muccioli, L.; Orlandi, S.; Zannoni, C. *Adv. Funct. Mater.* **2009**, *19*, 2592. (b) Shanker, G.; Nagaraj, M.; Kocot, A.; Vij, J. K.; Prehm, M.; Tschierske, C. *Adv. Funct. Mater.* **2012**, *22*, 1671. (c) Ghosh, S.;

Begum, N.; Turlapati, S.; Roy, S. Kr.; Das, A. Kr.; Rao, N. V. S. *J. Mater. Chem.* **2014**, *2*, 425.
(9) (a) Samulski, E. T. *Liq. Cryst.* **2010**, *37*, 669. (b) Vanakaras, A. G.; Photinos, D. J. *J. Chem. Phys.* **2008**, *128*, 154512. (c) Peroukidis, S. D.; Vanakaras, A. G.; Photinos, D. J. *Phys Rev. E* **2011**, *84*, 010702.
(10) (a) Vaupotič, N.; Szydlowska, J.; Salamonczyk, M.; Kovarova, A.; Svoboda, J.; Osipov, M.; Pociecha, D.; Gorecka, E. *Phys. Rev. E* **2009**, *80*, 030701. (b) Francescangeli, O.; Samulski, E. T. *Soft Matter* **2010**, *6*, 2413. (c) Francescangeli, O.; Vita, F.; Ferrero, C.; Dingemans, T.; Samulski, E. T. *Soft Matter* **2011**, *7*, 895. (d) Keith, C.; Lehmann, A.; Baumeister, U.; Prehm, M.; Tschierske, C. *Soft Matter* **2010**, *6*, 1704. (e) Hong, S. H.; Verduzco, R.; Williams, J. C.; Twieg, R. J.; DiMasi, E.; Pindak, R.; Jákli, A.; Gleeson, J. T.; Sprunt, S. *Soft Matter* **2010**, *6*, 4819. (f) Speetjens, F.; Lindborg, J.; Tauscher, T.; LaFemina, N.; Nguyen, J.; Samulski, E. T.; Vita, F.; Francescangeli, O.; Scharrer, E. *J. Mater. Chem.* **2012**, *22*, 22558. (g) Chakraborty, S.; Gleeson, J. T.; Jákli, A.; Sprunt, S. *Soft Matter* **2013**, *9*, 1817.
(11) (a) Laus, M.; Angeloni, A. S.; Galli, G.; Chiellini, E. *Macromolecules* **1992**, *25*, 5901. (b) Laus, M.; Righetti, M. C. *Macromolecules* **2001**, *34*, 7190.
(12) Achard, M. F.; Bedel, J. Ph.; Marceroua, J. P.; Nguyen, H. T.; Rouillon, J. C. *Eur. Phys. J. E* **2003**, *10*, 129.
(13) Monkade, M.; Boix, M.; Durand, G. *Europhys. Lett.* **1988**, *5*, 697.
(14) (a) Li, J.; Seok, S. I.; Chu, B.; Dogan, F.; Zhang, Q.; Wang, Q. *Adv. Mater.* **2009**, *21*, 217. (b) Hu, Z.; Tian, M.; Nysten, B.; Jonas, A. M. *Nat. Mater.* **2009**, *8*, 62. (c) Naber, R. C. G.; Asadi, K.; Blom, P. W. M.; de Leeuw, D. M.; de Boer, B. *Adv. Mater.* **2010**, *22*, 933. (d) Neese, B.; Chu, B.; Lu, S.-G.; Wang, Y.; Furman, E.; Zhang, Q. M. *Science* **2008**, *321*, 821. (e) Qian, X.-S.; Lu, S.-G.; Li, X.; Gu, H.; Chien, L.-C.; Zhang, Q. *Adv. Funct. Mater.* **2013**, *23*, 2894. (f) Chang, C.; Tran, V. H.; Wang, J.; Fuh, Y.-K.; Lin, L. *Nano Lett.* **2010**, *10*, 726.